

## COOL CORE CLUSTERS FROM COSMOLOGICAL SIMULATIONS

E. RASIA<sup>1,2</sup>, S. BORGANI<sup>1,3,4</sup>, G. MURANTE<sup>1</sup>, S. PLANELLES<sup>1,3,4</sup>, A. M. BECK<sup>5</sup>, V. BIFFI<sup>1,3</sup>, C. RAGONE-FIGUEROA<sup>6</sup>, G. L. GRANATO<sup>1</sup>, L. K. STEINBORN<sup>5</sup>, K. DOLAG<sup>5,7</sup>

<sup>1</sup> INAF, Osservatorio Astronomico di Trieste, via Tiepolo 11, I-34131, Trieste, Italy, rasia@oats.inaf.it

<sup>2</sup> Department of Physics, University of Michigan, 450 Church St., Ann Arbor, MI 48109, USA

<sup>3</sup> Dipartimento di Fisica dell' Università di Trieste, Sezione di Astronomia, via Tiepolo 11, I-34131 Trieste, Italy

<sup>4</sup> INFN, Istituto Nazionale di Fisica Nucleare, Trieste, Italy

<sup>5</sup> Universitäts-Sternwarte München, Scheinerstr.1, D-81679 München, Germany

<sup>6</sup> Instituto de Astronomía Teórica y Experimental (IATE), Consejo Nacional de Investigaciones Científicas y Técnicas de la República Argentina (CONICET), Observatorio Astronómico, Universidad Nacional de Córdoba, Laprida 854, X5000BGR, Córdoba, Argentina

<sup>7</sup> Max-Planck-Institut für Astrophysik, Karl-Schwarzschild Strasse 1, D-85740 Garching, Germany

*Draft version October 11, 2022*

### ABSTRACT

We present results obtained from a set of cosmological hydrodynamic simulations of galaxy clusters, aimed at comparing predictions with observational data on the diversity between cool-core and non-cool-core clusters. Our simulations include the effects of stellar and AGN feedback and are based on an improved version of the Smoothed-Particle-Hydrodynamics code GADGET-3, which ameliorates gas mixing and better captures gas-dynamical instabilities by including a suitable artificial thermal diffusion. In this *Letter*, we focus our analysis on the entropy profiles, our primary diagnostic to classify the degree of cool-core-ness of clusters, and on the iron profiles. In keeping with observations, our simulated clusters display a variety of behaviors in entropy profiles: they range from steadily decreasing profiles at small radii, characteristic of cool-core systems, to nearly flat core isentropic profiles, characteristic of non-cool-core systems. Using observational criteria to distinguish between the two classes of objects, we find them to occur in similar proportions in simulations and in observations. Furthermore, we also find that simulated cool-core clusters have profiles of iron abundance that are steeper than those of non-cool-core clusters, also in agreement with observational results. We show that the capability of our simulations to generate a realistic cool-core structure in the cluster population is due to AGN feedback and artificial thermal diffusion: their combined action allows to naturally distribute the energy extracted from super-massive black holes and to compensate the radiative losses of low-entropy gas with short cooling time residing in the cluster core.

*Subject headings:* galaxies: clusters: general – galaxies: clusters: intracluster medium – X-rays: galaxies: clusters – methods: numerical

### 1. INTRODUCTION

During their hierarchical assembly, galaxy clusters grow in mass via diffuse accretion processes as well as via violent merger events. These processes lead to shock heating the intra-cluster medium (ICM) to virial temperature of up to  $T \sim 10^8$  K, with central electron number densities corresponding to  $n_e \sim 10^{-3} \text{ cm}^{-3}$  (e.g. Voit 2005; Kravtsov & Borgani 2012, for a review). At this density, hot baryons in the core regions have a cooling time,  $t_{cool} \propto T^{1/2}/n_e$ , shorter than the Hubble time. Under this condition, the ICM suffers from radiative losses and becomes colder and denser. This process might initiate a run-away cooling process, which would cause an extreme accretion rate into the central galaxy, unless some heating mechanism balances the cooling. Substantial evidences from X-ray observations proved that the regulating mechanism is the feedback by active galactic nuclei (AGN, e.g. McNamara & Nulsen 2007; Voit et al. 2015).

In a situation of steady accretion, low-entropy gas associated to merging substructures or funneled by filaments sinks toward the core region. The gas accreted in clumps has been enriched in metals at higher levels with respect to the surrounding ICM, given its proximity to star-forming regions. Therefore, the gas in these cool cores (CC, named

as such by Molendi & Pizzolato 2001) is characterized by rather low entropy levels<sup>1</sup>, below  $50 \text{ keV cm}^2$ , and steep gradients of metal abundance (Vikhlinin et al. 2005). On the contrary, non-cool core (NCC) objects are observed with nearly isentropic gas cores at a higher entropy level and show no evidence of a spike in their metal abundance (De Grandi et al. 2004; Maughan et al. 2008; Böhringer & Werner 2010).

While idealized simulations reproduce some of the many feature of the CC systems (e.g. Li et al. 2015; Gaspari 2015), producing the diverse populations of CC and NCC clusters has proved to be so far quite a formidable challenge for cosmological hydrodynamic simulations (Borgani & Kravtsov 2011, and references therein). Earlier simulation works predicted that the origin of the two classes of CC and NCC clusters is “primeval”, with CC being destroyed exclusively by early mergers or preheating phenomena (Poole et al. 2008; McCarthy et al. 2008; Burns et al. 2008; Planelles & Quilis 2009). In fact, a CC cluster was claimed to maintain its high-density and metal-rich core even after a major merger, if that happens at

<sup>1</sup> We adopt here the definition of entropy which is standard in X-ray studies of galaxy clusters:  $K = T/n_e^{2/3}$  with  $T$  being the ICM temperature and  $n_e$  the electron number density.

$z \leq 0.5$ . However, this prediction is in tension with observations. In most cases CC clusters show regular X-ray morphology while the opposite is true for NCC systems (e.g. Sanderson et al. 2009). Data, thus, favor an “evolutionary” model in which a transition between CC and NCC status of a cluster can take place over relatively short timescales in consequence of a merger event that mixes the convective stable gas and destroys the CC (Rossetti et al. 2011). More recently, Dubois et al. (2011) were able to produce the correct CC entropy structure in a high-resolution simulation of a Virgo-like cluster by including the effect of AGN feedback. However, in the same paper these authors also claimed that this conclusion is spoiled as soon as the effect of metallicity is included in the cooling function. This confirms the fragility of a self-regulated AGN feedback that is able to produce CCs.

In this *Letter*, we present a set of simulated clusters in which for the first time we find: (i) co-existence of CC and NCC systems; (ii) agreement with the observed thermodynamical and chemical properties of the two classes of clusters; and (iii) evidence of recent transition between CC and NCC in the evolution of individual objects. As we will discuss, this result is achieved thanks to the combined action of a new AGN feedback model (Steinborn et al. 2015) and an improved SPH scheme (Beck et al. 2015) in which artificial conduction, among other features, allows Lagrangian hydrodynamics to better follow mixing processes.

## 2. SIMULATIONS

We provide a short description of the simulations analyzed here, while we refer to a forthcoming paper (Planelles et al., in preparation) for a more thorough description. The simulations have been generated from the same set of initial conditions originally presented by Bonafede et al. (2011). They correspond to zoomed-in initial conditions of 29 Lagrangian regions selected around 24 massive clusters with  $M_{200} > 8 \times 10^{14} h^{-1} M_{\odot}$  and 5 poorer clusters with  $M_{200}$  in the range  $1-4 \times 10^{14} h^{-1} M_{\odot}$ . The simulations are carried out with the GADGET-3 code (Springel 2005) and include an up-graded version of the SPH scheme, as described in Beck et al. (2015). These developments consist of: (a) a higher-order (Wendland  $C^4$  instead of the standard B-spline) interpolating kernel to better describe discontinuities and reduce clumpiness instability; (b) a time-dependent artificial viscosity term to minimize viscosity away from shock regions; (c) an artificial conduction term that largely improves the SPH capability of following gas-dynamical instabilities and mixing processes. The artificial conduction is applied to contact discontinuities in internal energy. With respect to the physical thermal conduction, it similarly promotes the transport of heat between particles, but differently it does not depend on the gas temperature. To assess the performances of this improved SPH implementation, several standard hydrodynamical tests, such as weak and strong shocks, shear flows, gas mixing, and self-gravitating gas, have been performed and presented in Beck et al. (2015).

The physical processes included in our simulations can be described as follows. Metallicity-dependent radiative cooling and the effect of a uniform time-dependent UV background are considered as in Planelles et al. (2014)

(see also Wiersma et al. 2009). A sub-resolution model for star formation from a multi-phase interstellar medium is implemented as in Springel & Hernquist (2003). Kinetic feedback driven by SN is accounted in the form of galactic winds with a velocity of  $v_w \sim 350 \text{ km s}^{-1}$ . Metal production from SN-II, SN-Ia and asymptotic-giant-branch (AGB) stars follows the original receipt by Tornatore et al. (2007) (see also Planelles et al. 2014). The AGN feedback is modeled with the implementations recently presented in Steinborn et al. (2015). The released thermal energy accounts for contributions by both mechanical outflows and radiation, separately computed in the code. Eddington-limited gas accretion onto BHs is computed by multiplying the Bondi rate by a boost factor  $\alpha$ . In this *Letter*, we consider only cold accretion ( $\alpha_{\text{cold}} = 100$  and  $\alpha_{\text{hot}} = 0$ ). For a subset of systems, we verified that the results hold when hot accretion is included with  $\alpha_{\text{hot}} = 10$ . In a future paper, we will investigate the effect on the evolution and properties of the central galaxy generated by varying the values of the two  $\alpha$  factors. As for the ensuing feedback energy, we assume variable efficiencies for the radiation and the mechanical outflow (Eq. 19 and 20 of Steinborn et al. 2015) that depend on the BH mass and on the accretion rate. Finally, we fix  $\epsilon_f = 0.05$  as the efficiency of coupling the radiated BH energy to the ICM.

We emphasize that parameters defining the modification of SPH and the AGN feedback model have been tuned to overcome the limitations of standard SPH in passing classic hydrodynamical tests and to reproduce the observational scaling relation between BH mass and stellar mass of the host galaxies, including the brightest cluster galaxies (McConnell & Ma 2013). No attempt has been pursued to reproduce any of the observational properties of the ICM.

## 3. RESULTS

Several approaches have been used in the literature to classify clusters as CC and NCC systems based, e.g., on the central gradient of temperature or entropy, on central entropy level, on the cooling time, on the mass deposition rate inferred from X-ray spectroscopy, on the cuspliness of the central gas density profile (comparisons among these criteria are presented in Cavagnolo et al. 2009; Leccardi et al. 2010; Hudson et al. 2010; McDonald et al. 2013; Pascut & Ponman 2015). In order to assign a degree of “cool-coreness” to our simulated clusters, we jointly use the following two criteria which measure the shape and level of the entropy profiles in the central regions and are extensively applied to observational data.

Following Rossetti et al. (2011, see also Leccardi et al. 2010), we base the first criterion on the computation of the pseudo entropy:

$$\sigma = \frac{(T_{\text{IN}}/T_{\text{OUT}})}{(EM_{\text{IN}}/EM_{\text{OUT}})^{1/3}}, \quad (1)$$

where the spectroscopic-like temperature (Mazzotta et al. 2004),  $T$ , and the emission measures,  $EM$ , are computed in the IN region,  $r < 0.05 \times R_{180}$ , and in the OUT region,  $0.05 \times R_{180} < r < 0.15 \times R_{180}$ . We define CC those clusters with  $\sigma < 0.55$ .

In addition, we request the value of the central entropy to be  $K_0 < 60 \text{ keV cm}^2$ . We model the entropy profile as

$$K = K_0 + K_{100} \times (R/R_{100k})^{\alpha}, \quad (2)$$

where we treat as free parameters the core entropy,  $K_0$ , the entropy at  $R_{100k}$  ( $= 100$  kpc),  $K_{100}$ , and the slope,  $\alpha$ , (Cavagnolo et al. 2009). For each simulated cluster the entropy profile is measured in linearly-equispaced spherical shells, with the innermost radius being that of the sphere containing the first 100 gas particles. In all cases, this radius is smaller than  $\sim 0.05 \times R_{500}$ . We use  $R_{500}$  as the outermost radius out to which perform the fit. Three clusters with  $\sigma < 0.55$  have steadily declining entropy profiles. In these cases,  $K_0$  is not constrained. We, thus, consider the overall profiles and keep in the CC sample the two objects with  $\alpha \sim 1$  and exclude that with  $\alpha < 0.5$ .

Finally, we find that 38% (11/29) of our simulated clusters at  $z = 0$  are classified as CC. This fraction is quite close to the 35% value reported by Eckert et al. (2011) from the HIGFLUGS sample after correcting for the bias that tends to enhance the CC fraction in an X-ray selected sample and for the incompleteness of the sample.

In the upper panels of Figure 1, we compare the entropy profiles of our simulated clusters with observational results obtained by Pratt et al. (2010) from XMM-Newton observations of the REXCESS clusters. Our simulations produce now a population of CC clusters, whose entropy profiles decline down to the innermost regions. This result confirms that the energy extracted from the central BHs is distributed in such a way to compensate radiative losses of gas at low entropy and, therefore, to keep it in the hot phase despite it formally has a short cooling time. More generally, we note that observed and simulated entropy profiles agree quite well in normalization and slope, for both CC and NCC populations.

In the bottom panels of the same figure, the simulated mass-weighted iron profiles are compared with the metallicity of nearby clusters,  $z < 0.2$ , from Ettori et al. (2015)<sup>2</sup>. In keeping with observational results, we find that CC clusters are characterized by a rather high enrichment level in the central regions while NCC objects have a shallower peak. This agreement witnesses that our simulations provide a correct *effective* description of the mixing related to gas-dynamical processes acting during the cluster formation and to the uplift of enriched gas caused by feedback processes: the same processes leading to the diversity of entropy profiles are also responsible for the diversity of the profiles of metal abundance.

From an object-by-object investigation of our simulated clusters, we recognize a variety of situations for the establishment of a CC and for the transformation between CC and NCC, which can take place over a quite short time and even at low redshift. As an example, in Figure 2 we show the evolution sequences of pseudo-entropy maps from  $z = 0.8$  to  $z = 0$  for two objects. Following an observational approach, we create maps of spectroscopic-like temperature,  $\mathcal{M}_{\text{TSL}}$ , and of X-ray soft band ([0.5-2] keV) emissivity,  $\mathcal{M}_{\text{X}}$ , which we then combine as  $\mathcal{M}_{\text{TSL}}/\mathcal{M}_{\text{X}}^{1/3}$  to build maps of pseudo entropy (Finoguenov et al. 2010). The upper panel shows the case of a NCC cluster at  $z = 0.8$  that later develops a CC structure. On the contrary, the

lower panel corresponds to a system with low-entropy core at high redshift. The core is still in place at  $z = 0.25$  and it is eventually destroyed by a merger between the main halo and a sub-clump at  $z \sim 0.1$ . Remarkably, this last case of CC remnant is not an isolated event: almost half of NCC clusters at  $z = 0$  were CC at  $z = 1$  (Rossetti et al. 2011).

These results are somewhat at variance with previous claims, also based on simulations, that CCs can only be destroyed at high redshift through major mergers, while being much more resilient against mergers at low redshift (e.g. Burns et al. 2008; Poole et al. 2008). A close comparison of our results with these previous analyses is not straightforward due to substantial differences in both the hydrodynamic schemes and the implementation of feedback. Poole et al. (2008) carried out non-cosmological simulations of isolated two-body mergers using a more standard implementation of SPH, while Burns et al. (2008) used an Eulerian code with cosmological set-up. Neither one of these two analyses included the effect of AGN feedback and, for this reason, the strength of their cores is probably affected by overcooling. In order to surpass this limitation, Burns et al. (2008) truncated star formation below a certain redshift, while Poole et al. (2008) excluded the central 40 kpc in their analysis. Both strategies, however, do not attack directly the main problem of the delicate balance between cooling and heating. This balance, essential for the creation of a low-entropy core, needs to be regulated since early times and can be achieved in our simulations only by including AGN feedback, as we will discuss below.

#### 4. DISCUSSION AND CONCLUSIONS

It is long known that ICM evolution purely driven by gravitational processes leads to self-similar entropy profiles that scale as a power-law of radius,  $K(r) \propto r^\alpha$  with  $\alpha \sim 1-1.1$  in the cluster outskirts (Voit et al. 2005; Nagai et al. 2007). Non-radiative simulations, however, differ on their behavior in the central regions. A flat core profile is found in grid-based codes (Frenk et al. 1999) and in recent improved versions of SPH (Biffi & Valdarnini 2015; Sembolini et al. 2015, and references therein). Standard SPH simulations, instead, produce entropy profiles that are declining towards the center.

In addition to mixing, radiative processes have the counterintuitive effect of also raising entropy in core regions (e.g. Borgani & Kravtsov 2011). If not counteracted by some energy feedback process, radiative cooling selectively removes gas with low entropy and short cooling time from the hot X-ray emitting phase, thus fuelling star formation (e.g. Li & Bryan 2012) and leaving in the ICM only gas with a relatively higher entropy.

The AGN feedback plays a key role to explain our results. Considering the new SPH set-up but excluding AGN feedback, we find that overcooling leads to a thermal structure of central cluster regions whose entropy profiles behave as in NCC clusters (top panel of Figure 3). At the same time, the excess of star formation produces an exceedingly high level of ICM metal enrichment, with heavy elements mostly locked around galaxies. As a consequence, simulated clusters without AGN always display spikes of central metallicity, enrichment pattern typical of CC clus-

<sup>2</sup> In their classification of CC/NCC clusters Ettori et al. (2015) use a slightly different definition of the IN and OUT regions for the pseudo-entropy calculation. Thus, for their clusters we consider the limit  $\sigma < 0.6$  that corresponds to our adopted threshold  $\sigma < 0.55$  according to Baldi et al. (2012).

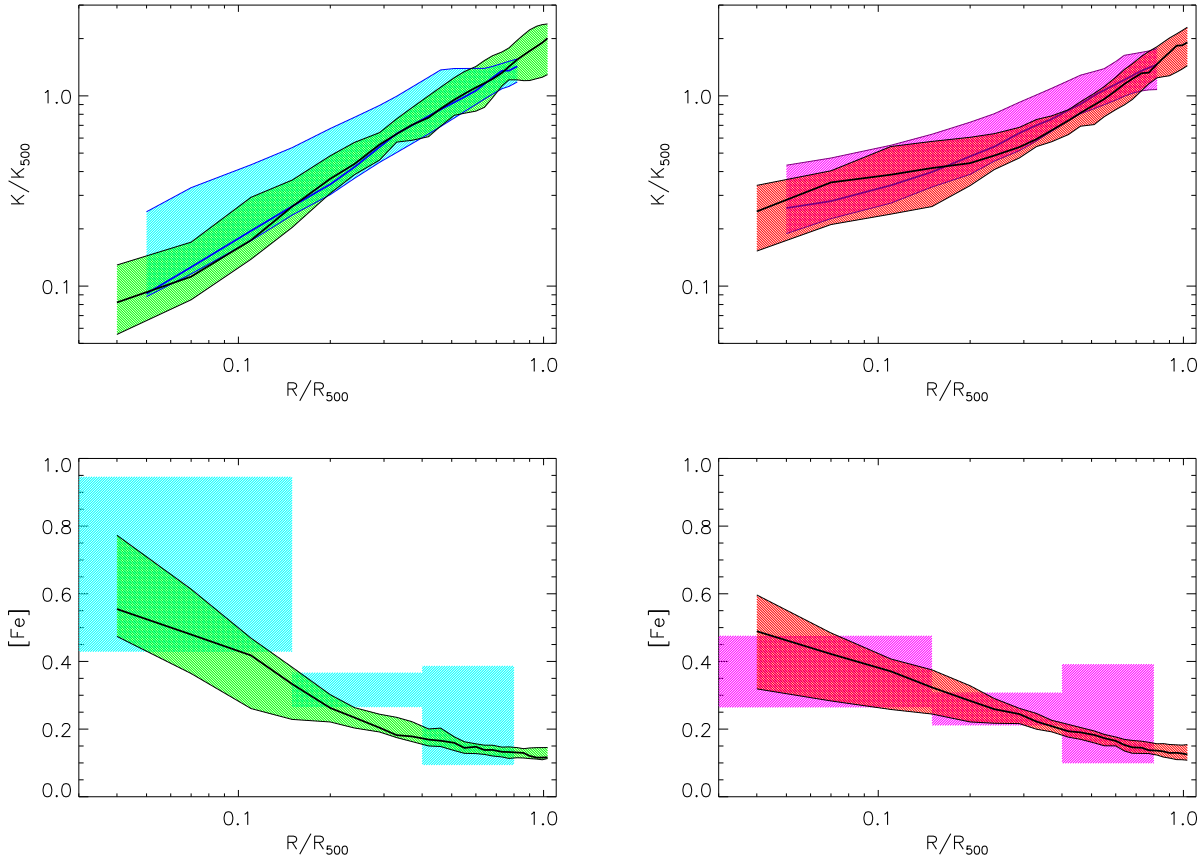


FIG. 1.— Simulated  $z = 0$  entropy (top panels) and Iron abundance (bottom panels) profiles compared with observations by Pratt et al. (2010) and by Ettori et al. (2015), respectively. The medians of the simulated CC (left panels) and NCC (right panels) profiles are in black. The shaded regions (in green and red, respectively) delimit the 16<sup>th</sup> and the 84<sup>th</sup> percentiles. The observed profiles for CC and NCC are, respectively, in cyan and magenta. Metallicity profiles are expressed in units of the solar abundance as reported by Anders & Grevesse (1989).

ters (bottom panel of Figure 3). As observations suggest, the AGN feedback should have the threefold effect of (i) compensating radiative losses so as to make gas with short cooling time not to drop out of the ICM; (ii) reducing star formation in massive halos at low redshift; (iii) uplifting metals away from star-forming regions (e.g. Fabjan et al. 2011; McCarthy et al. 2011).

However, attempts to create realistic thermal structures of CC in simulated clusters have so far failed, even when including AGN feedback, which is otherwise successful in reproducing X-ray scaling relations (e.g. Planelles et al. 2014; Le Brun et al. 2014, however, see also Ragne-Figueroa et al. 2013). The encouraging success of the simulations presented here in producing the correct thermal and chemo-dynamical structure of CC is related to the combined action of the AGN feedback model *and* of the artificial thermal diffusion.

Figure 4 compares the entropy profiles of the cluster shown in the upper panels of Figure 2 with those of the same object simulated without artificial conduction but including other recent implementations such as the new kernel and the artificial viscosity. Interestingly, by excluding artificial conduction, the entropy profiles at  $z = 0.8$  and  $z = 0$  are similar to each other with a large isentropic core, characteristics of a strongly NCC object. This contrast with the previous finding showing a transition from a

NCC to a CC situation (Figure 2). Besides confirming the results reported in previous works based on standard SPH (Sijacki et al. 2008; Planelles et al. 2014), this outcome highlights the role of artificial conduction in providing an effective description of the processes of mixing that lead to the redistribution of AGN feedback energy in central regions.

In summary, we showed that our simulations produce a population of clusters which have the correct CC structure, both from a thermo- and chemo-dynamical point of view. Furthermore, once this result is achieved, the simulations also naturally produce a mix of CC and NCC clusters which is similar to that observed. We trace the reason for the success of our simulations to the combined action of artificial conduction, introduced to overcome numerical limitations of standard SPH, and of AGN feedback, introduced to regulate star formation in massive halos.

As a concluding word of caution, we would like to emphasize that the success of the simulations presented here does not imply that we are self-consistently describing the details of all the physical processes that lead to the creation of cool cores: inflation of bubbles of high-entropy gas from the shocks of sub-relativistic jets launched by the AGN, gas circulation and turbulence triggered by the buoyancy of these bubbles, possible effects of magnetic

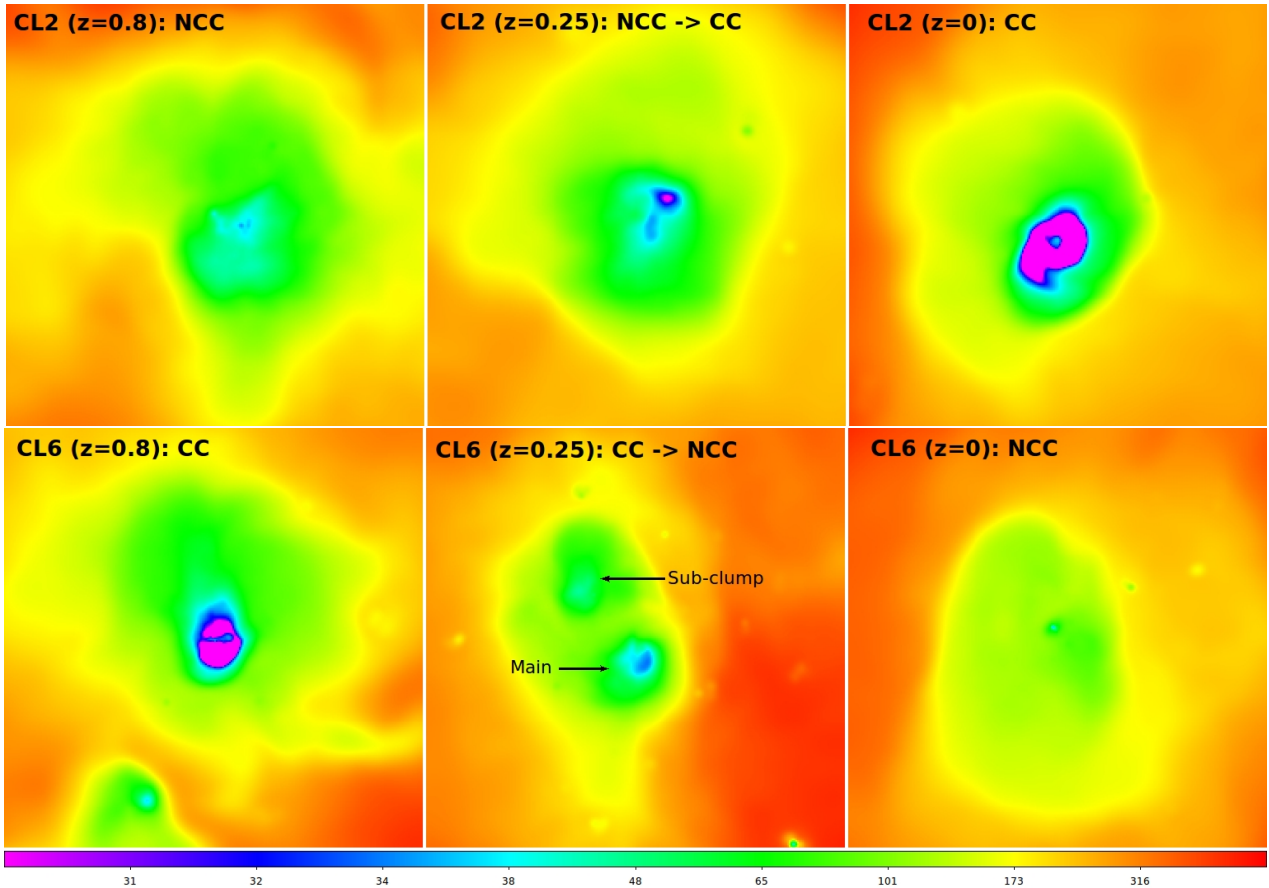


FIG. 2.— Maps of pseudo entropy of two simulated clusters that have masses  $M_{500} = 2.4 \times 10^{14} h^{-1} M_{\odot}$  (upper panels) and  $M_{500} = 7.3 \times 10^{14} h^{-1} M_{\odot}$  (lower panels) at  $z = 0$ . The size of the images is 1Mpc.

fields in stabilizing them, thermal conduction, cosmic rays. These are all effects for which we have circumstantial evidence from observations, but that are not included in our simulations. Still, our results demonstrate that our description of AGN feedback and artificial conduction provides a realistic *effective* description of the above physical processes, without requiring any specific fine tuning.

We are greatly indebted to D. Fabjan, V. Fiorenzo, M. Petkova, and L. Tornatore who contributed with the preparation of the simulations, and with D. Eckert, S. Ettori, A. Evrard, M. Gaspari, S. Molendi, P. Tozzi, M. Voit for useful discussions and comments. The authors thank Volker Springel for giving us access to the developer version of the GADGET3 code. We acknowledge financial support from: FP7-PEOPLE-2013-IIF (Grant Agreement PIIF-GA-2013-627474), NSF AST-1210973, PRIN-MIUR 201278X4FL, PRIN-INAF 2012 "The Universe in a Box: Multi-scale Simulations of Cosmic Structures", the INFN INDARK grant, "Consorzio per la Fisica" of Trieste, DFG Cluster of Excellence 'Universe', DFC Research Unit 1254, CONICET-Argentina, FonCyT. Simulations are carried out using Flux HCP Cluster at the University of Michigan efficiently supported by ARC-TS, and at CINECA (Italy), with CPU time assigned through ISCRAs proposals and through an agreement with the University of Trieste.

## REFERENCES

- Anders, E. & Grevesse, N. 1989, *Geochimica et Cosmochimica Acta*, 53, 197
- Baldi, A., Ettori, S., Molendi, S., & Gastaldello, F. 2012, *A&A*, 545, A41
- Beck, A. M., Murante, G., Arth, A., Remus, R.-S., Teklu, A. F., Donnert, J. M. F., Planelles, S., Beck, M. C., Foerster, P., Imgrund, M., Dolag, K., & Borgani, S. 2015, *ArXiv e-prints*
- Biffi, V., & Valdarnini, R. 2015, *MNRAS*, 446, 2802
- Böhringer, H., & Werner, N. 2010, *A&A Rev.*, 18, 127
- Bonafede, A., Dolag, K., Staszyszyn, F., Murante, G., & Borgani, S. 2011, *MNRAS*, 418, 2234
- Borgani, S. & Kravtsov, A. 2011, *Advanced Science Letters*, 4, 204
- Burns, J. O., Hallman, E. J., Gantner, B., Motl, P. M., & Norman, M. L. 2008, *ApJ*, 675, 1125
- Cavagnolo, K. W., Donahue, M., Voit, G. M., & Sun, M. 2009, *ApJS*, 182, 12
- De Grandi, S., Ettori, S., Longhetti, M., & Molendi, S. 2004, *A&A*, 419, 7
- Dubois, Y., Devriendt, J., Teyssier, R., & Slyz, A. 2011, *MNRAS*, 417, 1853
- Eckert, D., Molendi, S., & Paltani, S. 2011, *A&A*, 526, A79
- Ettori, S., Baldi, A., Balestra, I., Gastaldello, F., Molendi, S., & Tozzi, P. 2015, *A&A*, 578, A46
- Fabjan, D., Borgani, S., Rasia, E., Bonafede, A., Dolag, K., Murante, G., & Tornatore, L. 2011, *MNRAS*, 416, 801
- Finoguenov, A., Sanderson, A. J. R., Mohr, J. J., Bialek, J. J., & Evrard, A. 2010, *A&A*, 509, A85
- Frenk, C. S., White, S. D. M., Bode, P., Bond, J. R., Bryan, G. L., Cen, R., Couchman, H. M. P., Evrard, A. E., Gnedin, N., Jenkins, A., Khokhlov, A. M., Klypin, A., Navarro, J. F., Norman, M. L., Ostriker, J. P., Owen, J. M., Pearce, F. R., Pen, U.-L., Steinmetz, M., Thomas, P. A., Villumsen, J. V., Wadsley, J. W., Warren, M. S., Xu, G., & Yepes, G. 1999, *ApJ*, 525, 554
- Gaspari, M. 2015, *MNRAS*, 451, L60
- Hudson, D. S., Mittal, R., Reiprich, T. H., Nulsen, P. E. J., Andernach, H., & Sarazin, C. L. 2010, *A&A*, 513, A37
- Kravtsov, A. V., & Borgani, S. 2012, *ARA&A*, 50, 353

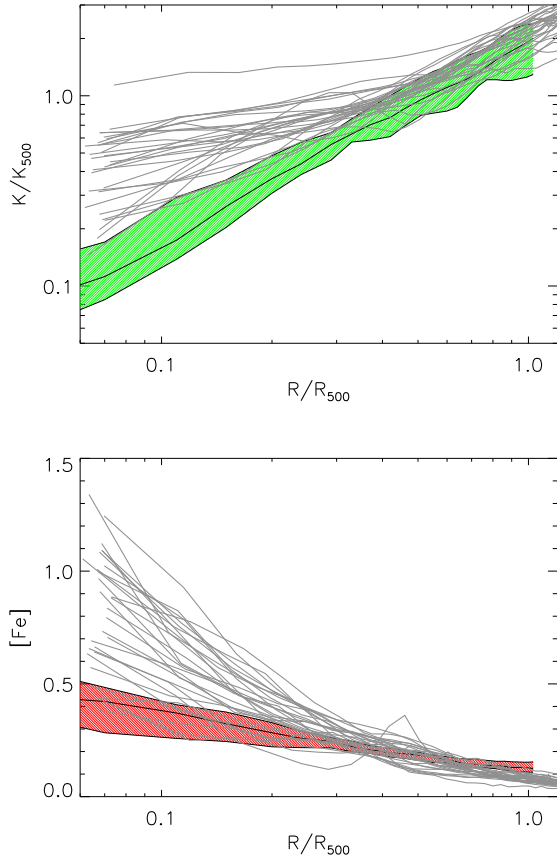


FIG. 3.— The effect of AGN feedback on entropy (upper panel) and iron abundance (lower panel) profiles for  $z = 0$  clusters. In each panel the grey lines show the profiles for each cluster in our set simulated without AGN feedback. In the upper panel, the green shaded area is for clusters classified as CC in the presence of AGN, while the red area in the lower panel is for the corresponding NCC clusters.

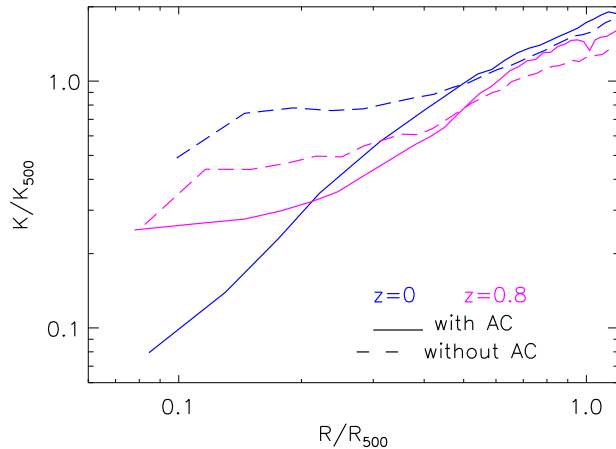


FIG. 4.— Effect of artificial conduction on the entropy profiles of the cluster shown in the upper panel of Fig. 2 at two instances:  $z = 0.8$  (magenta curves) and  $z = 0$  (blue curves). The simulation has been carried out with and without artificial conduction (solid and dashed lines, respectively), while leaving all the other parameters unchanged. The cluster simulated with artificial conduction was classified NCC and CC at the two epochs.

- Le Brun, A. M. C., McCarthy, I. G., Schaye, J., & Ponman, T. J. 2014, *MNRAS*, 441, 1270
- Leccardi, A., Rossetti, M., & Molendi, S. 2010, *A&A*, 510, A82
- Li, Y. & Bryan, G. L. 2012, *ApJ*, 747, 26
- Li, Y., Bryan, G. L., Ruszkowski, M., et al. 2015, arXiv:1503.02660
- Maughan, B. J., Jones, C., Forman, W., & Van Speybroeck, L. 2008, *ApJS*, 174, 117
- Mazzotta, P., Rasia, E., Moscardini, L., & Tormen, G. 2004, *MNRAS*, 354, 10
- McCarthy, I. G., Babul, A., Bower, R. G., & Balogh, M. L. 2008, *MNRAS*, 386, 1309
- McCarthy, I. G., Schaye, J., Bower, R. G., et al. 2011, *MNRAS*, 412, 1965
- McConnell, N. J., & Ma, C.-P. 2013, *ApJ*, 764, 184
- McDonald, M., Benson, B. A., Vikhlinin, A., Stalder, B., Bleem, L. E., de Haan, T., Lin, H. W., Aird, K. A., Ashby, M. L. N., Bautz, M. W., Bayliss, M., Bocquet, S., Brodwin, M., Carlstrom, J. E., Chang, C. L., Cho, H. M., Clocchiatti, A., Crawford, T. M., Crites, A. T., Desai, S., Dobbs, M. A., Dudley, J. P., Foley, R. J., Forman, W. R., George, E. M., Gettings, D., Gladders, M. D., Gonzalez, A. H., Halverson, N. W., High, F. W., Holder, G. P., Holzappel, W. L., Hoover, S., Hrubes, J. D., Jones, C., Joy, M., Keisler, R., Knox, L., Lee, A. T., Leitch, E. M., Liu, J., Lueker, M., Luong-Van, D., Mantz, A., Marrone, D. P., McMahon, J. J., Mehl, J., Meyer, S. S., Miller, E. D., Mocanu, L., Mohr, J. J., Montroy, T. E., Murray, S. S., Nurgaliev, D., Padin, S., Plagge, T., Pryke, C., Reichardt, C. L., Rest, A., Ruel, J., Ruhl, J. E., Saliwanchik, B. R., Saro, A., Sayre, J. T., Schaffer, K. K., Shirokoff, E., Song, J., Šuhada, R., Spieler, H. G., Stanford, S. A., Staniszewski, Z., Stark, A. A., Story, K., van Engelen, A., Vanderlinde, K., Vieira, J. D., Williamson, R., Zahn, O., & Zenteno, A. 2013, *ApJ*, 774, 23
- McNamara, B. R. & Nulsen, P. E. J. 2007, *ARA&A*, 45, 117
- Molendi, S. & Pizzolato, F. 2001, *ApJ*, 560, 194
- Nagai, D., Kravtsov, A. V., & Vikhlinin, A. 2007, *ApJ*, 668, 1
- Pascut, A. & Ponman, T. J. 2015, *MNRAS*, 447, 3723
- Planelles, S., & Quilis, V. 2009, *MNRAS*, 399, 410
- Planelles, S., Borgani, S., Fabjan, D., Killeddar, M., Murante, G., Granato, G. L., Ragone-Figueroa, C., & Dolag, K. 2014, *MNRAS*, 438, 195
- Poole, G. B., Babul, A., McCarthy, I. G., Sanderson, A. J. R., & Fardal, M. A. 2008, *MNRAS*, 391, 1163
- Pratt, G. W., Arnaud, M., Piffaretti, R., Böhringer, H., Ponman, T. J., Croston, J. H., Voit, G. M., Borgani, S., & Bower, R. G. 2010, *A&A*, 511, A85
- Ragone-Figueroa, C., Granato, G. L., Murante, G., Borgani, S., & Cui, W. 2013, *MNRAS*, 436, 1750
- Rossetti, M., Eckert, D., Cavalleri, B. M., Molendi, S., Gastaldello, F., & Ghizzardi, S. 2011, *A&A*, 532, A123
- Sanderson, A. J. R., Edge, A. C., & Smith, G. P. 2009, *MNRAS*, 398, 1698
- Sembolini, F., Yepes, G., Pearce, F. R., Knebe, A., Kay, S. T., Power, C., Cui, W., Beck, A. M., Borgani, S., Dalla Vecchia, C., Davé, R., Jahan Elahi, P., February, S., Huang, S., Hobbs, A., Katz, N., Lau, E., McCarthy, I. G., Murante, G., Nagai, D., Nelson, K., Newton, R. D. A., Puchwein, E., Read, J. I., Saro, A., Schaye, J., & Thacker, R. J. 2015, *ArXiv e-prints*
- Sijacki, D., Pfrommer, C., Springel, V., & Enßlin, T. A. 2008, *MNRAS*, 387, 1403
- Springel, V. 2005, *MNRAS*, 364, 1105
- Springel, V., & Hernquist, L. 2003, *MNRAS*, 339, 289
- Steinborn, L. K., Dolag, K., Hirschmann, M., Prieto, M. A., & Remus, R.-S. 2015, *MNRAS*, 448, 1504
- Tornatore, L., Borgani, S., Dolag, K., & Matteucci, F. 2007, *MNRAS*, 382, 1050
- Vikhlinin, A., Markevitch, M., Murray, S. S., et al. 2005, *ApJ*, 628, 655
- Voit, G. M. 2005, *Reviews of Modern Physics*, 77, 207
- Voit, G. M., Donahue, M., Bryan, G. L., & McDonald, M. 2015, *Nature*, 519, 203
- Voit, G. M., Kay, S. T., & Bryan, G. L. 2005, *MNRAS*, 364, 909
- Wiersma, R. P. C., Schaye, J., & Smith, B. D. 2009, *MNRAS*, 393, 99